

ON THE CO-ORBITAL MOTION IN THE PLANAR RESTRICTED THREE-BODY PROBLEM: THE QUASI-SATELLITE MOTION REVISITED

ALEXANDRE POUSSE, PHILIPPE ROBUTEL, AND ALAIN VIENNE

ABSTRACT. In the framework of the planar and circular Restricted Three-Body Problem, we consider an asteroid that orbits the Sun in quasi-satellite motion with a planet. A quasi-satellite trajectory is a heliocentric orbit in co-orbital resonance with the planet, characterized by a non zero eccentricity and a resonant angle that librates around zero. Likewise, in the rotating frame with the planet it describes the same trajectory as the one of a retrograde satellite even though the planet acts as a perturbator.

In the last few years, the discoveries of asteroids in this type of motion made the term “quasi-satellite” more and more present in the literature. However, some authors rather use the term “retrograde satellite” when referring to this kind of motion in the studies of the restricted problem in the rotating frame.

In this paper we intend to clarify the terminology to use, in order to bridge the gap between the perturbative co-orbital point of view and the more general approach in the rotating frame. Through a numerical exploration of the co-orbital phase space, we describe the quasi-satellite domain and highlight that it is not reachable by low eccentricities by averaging process. We will show that the quasi-satellite domain is effectively included in the domain of the retrograde satellites and neatly defined in terms of frequencies.

Eventually, we highlight a remarkable high eccentric quasi-satellite orbit corresponding to a frozen ellipse in the heliocentric frame. We extend this result to the eccentric case (planet on an eccentric motion) and show that two families of frozen ellipses originate from this remarkable orbit.

Restricted Three-Body Problem and Co-orbital motion and Quasi-satellite and Averaged Hamiltonian

1. INTRODUCTION

Following the discoveries, in 1899 and 1908, of the retrograde moons Phoebe and Pasiphea moving at great distances from their respective primaries Saturn and Jupiter, Jackson (1913) published the first study dedicated to the motion of the retrograde satellites (RS). Seeking to understand how a moon could still be satellized at this remote distance (close to the limit of the planet Hill’s sphere), he highlighted in the Sun-Jupiter system that

IMCCE, OBSERVATOIRE DE PARIS, UPMC UNIV. PARIS 6, UNIV. LILLE 1, CNRS, 77 AV. DENFERT-ROCHEREAU, 75014 PARIS, FRANCE

E-mail addresses: alexandre.pousse@obspm.fr, philippe.robutel@obspm.fr, alain.vienne@obspm.fr.

Date: June 15, 2019.

where “[...] the solar forces would prohibited direct motion, [...] the solar and the Jovian forces would go hand in hand to maintain a retrograde satellites”. Thus, by this remark the author was the first to confirm the existence and stability of remote retrograde satellite objects in the solar system. Afterwards, the existence and stability of some retrograde satellite orbits far from the secondary body have also been established in the planar Restricted Three-Body Problem (RTBP) with two equal masses (Strömgren, 1933; Moeller, 1935; Henon, 1965a,b)¹ and in the Earth-Moon system (Broucke, 1968).

In the framework of the Hill’s approximation, Henon (1969) extended Jackson’s study and highlighted that there exists a one-parameter family of stable retrograde satellite periodic orbits (denoted family f) that could exists beyond the Eulerian configurations L_1 and L_2 . This has been confirm in Henon and Guyot (1970) in the Restricted Three-Body Problem. The authors showed in the rotating frame with the planet (RF), that the family f extends from the retrograde satellite orbits in an infinitesimal neighbourhood of the secondary to the collision orbit with the primary. Besides, they pointed out that if ε , the ratio of the secondary mass over the sum of the system masses, is less than 0.0477, the whole family is stable. Benest (1974, 1975, 1976) extended these results by studying the stability of the neighbourhood of the family f in the configuration space for $0 \leq \varepsilon \leq 1$.

After these theoretical works, the study of the retrograde satellite orbits was addressed in a more practical point of view, with the project to inject a spacecraft in a circum-Phobos orbit. Remark that as the Phobos Hill’s sphere is too close to its surface, remote retrograde satellites are particularly adapted trajectories. Hence, at the end of the eighties, the terminology “Quasi-satellite”² (QS) appeared in the USSR astrodynamist community to define trajectories in the Restricted Three-Body Problem in rotating frame that correspond to retrograde satellite orbits outside the Hill’s sphere of the secondary body (see Fig.1a). The Phobos mission study led to the works of Kogan (1990) and Lidov and Vashkov’yak (1993, 1994a,b).

At the end of the nineties, the quasi-satellite motion appeared in the celestial mechanics community in the view of asteroid trajectories in the solar system. Let us suppose a QS-type asteroid far enough from the planet so that the influence of the Sun dominates its movement and therefore that the planet acts as a perturbator. Then, its trajectory could be represented by heliocentric osculating ellipses whose variations are governed by the influence of the planet. In this context, Mikkola and Innanen (1997) remarked that the asteroid and the planet are in 1 : 1 mean motion resonance and therefore that the quasi-satellite orbits correspond to a particular kind of configurations in the co-orbital resonance. Unlike the tadpole (TP) orbits that librate around the Lagrangian equilibria L_4 and L_5 or the horseshoes (HS) that encompass L_3 , L_4 and L_5 , the quasi-satellite orbits

¹ The two firsts are works of the Copenhagen group that extensively explored periodic orbit solutions in the planar Restricted Three-Body Problem with two equal masses. The two lasts are the first numerical explorations of all the solutions of the Restricted Three-Body Problem that recovered and completed the precedent works.

² Let us still mention that the “quasi-satellite” terminology has already been used in the paper of Danielsson and Ip (1972) but this was to describe the resonant behaviour of the near-Earth Object 1685 Toro and therefore was completely disconnected to retrograde satellite motion.

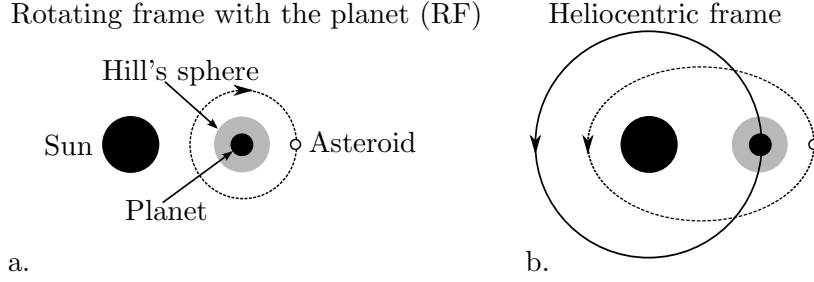


FIGURE 1. Asteroid on a quasi-satellite orbit (QS). In the rotating frame with the planet (RF) (a.), the trajectory is those of a retrograde satellite (RS) outside the planet Hill's sphere. In the heliocentric frame (b.), the trajectory is represented by heliocentric osculating ellipses with a non zero eccentricity (in the circular case) and $\theta = \lambda - \lambda'$ that librates around zero.

are characterized by a resonant angle $\theta = \lambda - \lambda'$ that librates around zero (where λ and λ' are the mean longitudes of the asteroid and the planet) and a non zero eccentricity if the planet gravitates on a circle (see Fig.1b). In their paper, these authors also described a first perturbative treatment to study the long term stability of quasi-satellites in the solar system. At that time no natural object was known to orbit this configuration. However, they suggested that, at least, the Earth and Venus could have quasi-satellite companions. Following this work, Wiegert et al. (2000) also predicted, via a numerical investigation of the stability around the giant planets, that Uranus and Neptune could harbour QS-type asteroids whereas they did not found stable solutions for Jupiter and Saturn. Subsequently, Namouni (1999) and Namouni et al. (1999) became the reference in term of co-orbital dynamics with close encounters. Using Hill's approximation, these authors highlighted that in the spatial case, transitions between horseshoe and quasi-satellite trajectories could occurred. They exhibited new kinds of compound trajectories denoted HS-QS, TP-QS or TP-QS-TP which means that there exists stable transitions exit between quasi-satellite, tadpole and horseshoe orbits. Later, Nesvorný et al. (2002) recovered these new co-orbital structures in a global study of the co-orbital resonance phase space. By developing a perturbative scheme using numerical averaging techniques, they showed how the tadpole, horseshoe, quasi-satellite and compound orbits vary with the asteroid eccentricity and inclination in the planar-circular, planar-eccentric and spatial-circular models. Particularly, they showed that the higher the asteroid's eccentricity is, the larger the domain occupied by the quasi-satellite orbits in the phase space is. Eventually, the quasi-satellite long-term stability has been studied using perturbation theory in Mikkola et al. (2006) and Sidorenko et al. (2014). The first ones developed a practical algorithm to detect QS-type asteroids on temporary or perpetual regime, while the last ones established conditions of existence of quasi-satellite motion and also explore its different possible regimes.

Following these theoretical works, many objects susceptible to be at least temporary quasi-satellites have been found in the solar system. The first confirmed minor body was 2002 VE68 in co-orbital motion with Venus in Mikkola et al. (2004). The Earth (Brasser et al., 2004; Connors et al., 2002, 2004; de la Fuente Marcos and de la Fuente Marcos, 2014; Wajer, 2009, 2010) and Jupiter (Kinoshita and Nakai, 2007; Wajer and Królikowska, 2012) are the two planets with the largest number of documented QS-type objects. Likewise, Saturn (Gallardo, 2006), Uranus (Gallardo, 2006; de la Fuente Marcos and de la Fuente Marcos, 2014), Neptune (de la Fuente Marcos and de la Fuente Marcos, 2012) possess at least one of this type.

At last, let us mention that quasi-satellite motion could play a role in other celestial problems: according to Kortenkamp (2005) and (2013), planetesimals could be trapped in quasi-satellite motion around the protoplanet as well as interplanetary dust particles around Earth. Eventually, although no co-orbital exoplanet system has been found, several studies on the planetary Three-Body Problem (TBP) showed the existence and the stability of two co-orbital planets in quasi-satellite motion (Hadjidemetriou et al., 2009; Hadjidemetriou and Voyatzis, 2011; Giuppone et al., 2010).

During these last twenty years, even though the “quasi-satellite” terminology becomes dominant in the literature, some studies use rather “retrograde satellite” (Namouni, 1999; Nesvorný et al., 2002) in reference to the neighbourhood of the family f in the restricted problem in rotating frame. Hence, there exists an ambiguity in terms of terminology that is a consequence of the several approaches to describe these orbits, depending on the distance between the two co-orbitals. One of our purposes is thus to clarify the terminology to use between “quasi-satellite” and “retrograde satellite”. Then, we chose to revisit the classical works on the family f (Henon and Guyot, 1970; Benest, 1974) in the section 4 and through a study on its frequencies, we show that the neighbourhood of the family is split in three different domains connected by an orbit; one corresponding to the “satellized” retrograde satellite orbits while the two others to the quasi-satellites. Among these two quasi-satellite domains, we identify one that is associated with asteroid trajectories in the solar system. This is on this last one that the paper is focussed.

An usual approach for these co-orbital trajectories in the restricted (Mikkola et al., 2006; Nesvorný et al., 2002; Sidorenko et al., 2014) and planetary (Robutel and Pousse, 2013) problems consists on averaging the Hamiltonian over the fast angle of the system (the planet mean longitude) to reduce the study of the problem to its semi-fast and secular components. This approach is generally denoted as the averaged problem (AP). However, as mentioned in Robutel and Pousse (2013) and Robutel et al. (2015), this one has the important drawback to reflect poorly the dynamics close to the singularity associated with the collision with the planet. Some quasi-satellite trajectories having close encounter with the planet, these are located close to the singularity in the averaged problem which implies that this approach would not be appropriate for them. Thus, in order to estimate a validity limit of the averaged problem for the study of quasi-satellite motion, we also revisit the co-orbital resonance via the averaged problem.

Firstly, in the section 2, we develop the Hamiltonian formalism of the problem and introduce the averaged problem. Subsequently, in the section 3, we focus on the circular

case that allows possible reduction. We introduce the reduced averaged problem (RAP) that seems to be the most adapted approach to understand the dynamics in the co-orbital resonance. Focussing on quasi-satellite motion, we exhibit a family of fixed points in the reduced averaged problem representing the family f that allows us to estimate the validity limit of the averaged problem.

Next, to bridge a gap between the averaged problem and the works of Henon and Guyot (1970) and Benest (1975), we devote the section 4 to revisit the motion in the rotating frame in the circular case in order to describe the family f as well as its reachable part in the averaged problem and characterize its neighbourhood. Through this study, we show how the quasi-satellite domain reachable in the averaged problem shrinks by increasing ε .

At last, in the section 5, we come back to the averaged problem with the aim to extend in the eccentric case (i.e. planet on an eccentric orbit) a result on co-orbital frozen orbits that has been highlighted in section 3.4.

2. THE AVERAGED PROBLEM

In the framework of the planar RTBP, we consider a primary with a mass $1 - \varepsilon$ (the Sun or a star), a secondary (a planet) with a mass ε small with respect to 1 and a massless third body (particle or asteroid). We assume that the planet is in elliptic Keplerian motion whose eccentricity is denoted e' . Without loss of generality, we set that its semi-major axis is equal to 1 and that the argument of its periaster is equal to zero. In an heliocentric frame, the Hamiltonian of the problem reads

$$(1) \quad H(\mathbf{r}, \dot{\mathbf{r}}, t) = H_0(\mathbf{r}, \dot{\mathbf{r}}) + \varepsilon H_1(\mathbf{r}, \dot{\mathbf{r}}, t)$$

with

$$(2) \quad \begin{aligned} H_0(\mathbf{r}, \dot{\mathbf{r}}) &= \frac{1}{2} \|\dot{\mathbf{r}}\|^2 - \frac{1}{\|\mathbf{r}\|} \quad \text{and} \\ H_1(\mathbf{r}, \dot{\mathbf{r}}, t) &= -\frac{1}{\|\mathbf{r} - \mathbf{r}'(t)\|} + \frac{1}{\|\mathbf{r}\|} + \frac{\langle \mathbf{r}, \mathbf{r}'(t) \rangle}{\|\mathbf{r}'(t)\|^3}. \end{aligned}$$

In this expression, \mathbf{r} is the heliocentric position of the particle, $\dot{\mathbf{r}}$ its conjugated variable and $\mathbf{r}'(t)$ is the position of the planet at the time t . In order to define a canonical coordinate system related to the elliptic elements (a, e, λ, ω) (respectively semi-major axis, eccentricity, mean longitude and argument of the periaster), we start from Poincaré's variables in complex form $(\lambda, \Lambda, x, -i\bar{x})$ where $\Lambda = \sqrt{a}$, $\Gamma = \Lambda(1 - \sqrt{1 - e^2})$ and $x = \sqrt{\Gamma} \exp(i\omega)$. In order to work with an autonomous Hamiltonian, we extend the phase space by introducing Λ' , the conjugated variable of $\lambda' = n't$, n' being the planet's mean motion. As a consequence the Hamiltonian becomes, on the extended phase space, equal to $H + n'\Lambda'$. Focussing on the co-orbital resonance, we introduce the new canonical coordinates $(\theta, u, x, -i\bar{x}, \lambda', \tilde{\Lambda}')$ where

$$(3) \quad \theta = \lambda - \lambda' \quad , \quad u = \sqrt{a} - 1 \quad \text{and} \quad \tilde{\Lambda}' = \Lambda' + \Lambda,$$

the variables x and $-i\bar{x}$ being unchanged. In what follows, the canonical transformation that maps the coordinate system $(\theta, u, x, -i\bar{x}, \lambda', \tilde{\Lambda}')$ to $(\mathbf{r}, \dot{\mathbf{r}}, \lambda', \Lambda')$ will be denoted by ϕ .

As inside the co-orbital resonance, the angle θ varies slowly with respect to the planet mean longitude, we chose to average the Hamiltonian over the fast angle λ' to reduce the dimension of the problem. The averaged Hamiltonian will be denoted \overline{H} .

2.1. The averaged Hamiltonian. According to the perturbation theory, there exists a canonical transformation \mathcal{C} , close to the identity, such that

$$(4) \quad (n'\Lambda' + H) \circ \phi \circ \mathcal{C} = n'\tilde{\Lambda}' + \overline{H} + \mathcal{O}(\varepsilon^2).$$

In the averaged variables defined as

$$(5) \quad (\theta, u, x, -i\bar{x}, \lambda', \dot{\lambda}') = \mathcal{C}^{-1}(\theta, u, x, -i\bar{x}, \lambda', \dot{\lambda}'),$$

\overline{H} reads:

$$(6) \quad \overline{H}(\theta, u, x, -i\bar{x}) = -n'(1+u) - \frac{1}{2(1+u)^2} + \varepsilon \overline{H}_1(\theta, u, x, -i\bar{x})$$

with

$$(7) \quad \overline{H}_1(\theta, u, x, -i\bar{x}) = \frac{1}{2\pi} \int_0^{2\pi} (H_1 \circ \phi)(\theta, u, x, -i\bar{x}, \lambda', \dot{\lambda}') d\lambda'.$$

If $\{f, g\}$ represents the Poisson bracket of the two functions f and g and if y stands for one of the variables $(\theta, u, x, -i\bar{x}, \lambda', \dot{\lambda}')$, the two coordinate systems are related by

$$(8) \quad y = y + \varepsilon \{W, y\} + \mathcal{O}(\varepsilon^2) \quad \text{with} \quad W = \frac{1}{n'} \int_0^{\lambda'} (\overline{H}_1 - H_1 \circ \phi) d\lambda'$$

Thus, the averaged Hamiltonian \overline{H} processes two degrees of freedom and depends on one parameter, the planetary eccentricity e' . For the sake of clarity, the “underdot” used to denote the averaged coordinates will be omitted.

2.2. Numerical averaging. There exists at least two classical averaging techniques adapted to the co-orbital resonance: an analytical one based on an expansion of the Hamiltonian in power series of the eccentricity (e.g. Morais, 2001; Robutel and Pousse, 2013), and a numerical one consisting on a numerical evaluation of \overline{H} and its derivatives (e.g. Nesvorný et al., 2002; Giuppone et al., 2010; Beaugé and Roig, 2001; Mikkola et al., 2006; Sidorenko et al., 2014). Whereas for low eccentricities the analytical technique is very efficient, reaching higher values of eccentricity requires high order expansions which generate very heavy expressions. Thus, in this case, the use of numerical methods may be more convenient. Then in order to explore the phase space of the co-orbital resonance for all eccentricities lower than one, we use the numerical averaging method developed by Nesvorný et al. (2002).

This method consists on a numerical evaluation of the integral (7). More generally, let F be a generic function depending on $(\theta, u, x, -i\bar{x}, E, E')$ where E and E' are the eccentric anomaly of the particle and the planet. As its average over the mean longitude λ' is computed for a given fixed value of θ , we have $d\lambda' = d\lambda = (1 - e \cos E) dE$. As

$$(9) \quad \theta = \lambda - \lambda' = E + \omega - E' - e \sin E + e' \sin E',$$

the eccentric anomalies E' can be expressed in terms of $(\theta, E, \omega, e, e')$. Eventually, the integrals reads

$$(10) \quad \overline{F}(\theta, u, x, -i\bar{x}) = \frac{1}{2\pi} \int_0^{2\pi} F(\theta, u, x, -i\bar{x}, E, E'(\theta, E, \omega, e, e'))(1 - e \cos E) dE,$$

which can be computed by discretizing the variable E as $E_k = \frac{k2\pi}{N}$ and $100 \leq N \leq 300$ (see Nesvorný et al., 2002, for more details).

3. THE CO-ORBITAL RESONANCE IN THE CIRCULAR CASE ($e' = 0$)

In the circular case, the “averaged problem” (AP) – defined by \overline{H} – being invariant under the action of the symmetry group $SO(2)$ associated with the rotations around the vertical axis, we have

$$(11) \quad \frac{\partial \overline{H}}{\partial \omega}(\theta, u, x, -i\bar{x}) = 0 = \dot{x}\bar{x} + x\dot{\bar{x}} = \dot{\Gamma},$$

which imposes Γ to be a first integral. As a consequence, in the averaged problem, the two degrees of freedom of the problem are separable and a reduction is possible. Thus, by fixing the value of the parameter Γ and eliminating the cyclic variable ω , we suppress one degree of freedom. We call this new problem the “reduced averaged problem” (RAP). However, instead of using the parameter Γ , it is more convenient to introduce the quantity $e_0 := \sqrt{1 - (1 - \Gamma)^2}$, which is equal to e for $u = 0$.

3.1. The reduced Hamiltonian. For a fixed value $e_0 = \zeta$ such that $0 \leq \zeta < 1$, let us define $\overline{\mathcal{M}}_{e_0}$ the intersection of the phase space of the averaged problem denoted $\overline{\mathcal{M}}$ with the hyperplane $\{e_0 = \zeta\}$, and $\overline{\mathcal{M}}_{e_0}/SO(2)$, the quotient space of this section by the symmetry group $SO(2)$. Under the action of the application

$$(12) \quad \begin{array}{ccc} \psi_{e_0} : & \overline{\mathcal{M}}_{e_0} & \rightarrow \overline{\mathcal{M}}_{e_0}/SO(2) \\ & (\theta, u, \omega) & \mapsto (\theta, u), \end{array}$$

the problem is reduced to one degree of freedom and is associated with the reduced Hamiltonian $\overline{H}_{e_0} := \overline{H}(\cdot, \cdot, \Gamma(e_0))$. Thus, for a fixed e_0 , a trajectory in the RAP is generally a periodic orbit, but can also be a fixed point. As a consequence, the description of the RAP’s phase portrait obtained for various values of e_0 allows to understand the global dynamics of the co-orbital resonance for $e' = 0$. The AP being more usual to illustrate the semi-fast and secular variations of the orbital elements and the rotating frame (RF) more classic to understand the dynamics of the RTBP, we will see in the next section how a given orbit is represented in these three different points of view.

3.2. Correspondence between the RAP, the AP and the RF. Let us consider, a periodic trajectory of frequency ν in the RAP. Its frequency being of order $\sqrt{\varepsilon}$ (see Mikkola et al., 2006), then it is associated with the semi-fast component of the dynamics.

The correspondence between the RAP and the AP consists in the pullback of a trajectory belonging to $\overline{\mathcal{M}}_{e_0}/SO(2)$ by the application $\psi_{e_0}^{-1}$. However, ω being ignorable in the RAP, $\psi_{e_0}^{-1}$ is not an injection, which implies that a family of orbits in the AP parametrized by

$\omega(0) \in [0, 2\pi]$ is mapped by ψ_{e_0} to the initial trajectory. For each orbits of the family, the temporal evolution of the argument of its periastrer is given by

$$(13) \quad \omega(t) = \omega(0) + gt + \int_0^t \left(-\frac{\partial}{\partial \Gamma} \overline{H}_{e_0}(\theta(t), u(t)) - g \right) dt$$

where

$$(14) \quad g = \frac{\nu}{2\pi} \int_0^{2\pi/\nu} -\frac{\partial}{\partial \Gamma} \overline{H}_{e_0}(\theta(t), u(t)) dt$$

is the secular precession frequency of ω . As a consequence, a given periodic trajectory in the RAP generally corresponds, in the AP, to a family of quasi-periodic orbits of frequencies ν and g . Nevertheless, let us mention that when the osculating ellipses are circles ($e_0 = 0$), ω being ignorable, the trajectories are fixed points or periodic orbits of frequency ν in both approaches. Likewise when $e_0 > 0$ and $g = 0$, a periodic trajectory of the RAP provides a family of periodic orbits of frequency ν in the AP while a fixed point corresponds to a family of degenerated fixed points.

Next, to connect the AP with the RF, we firstly have to apply \mathcal{C} to the trajectory (i.e. inverse the equation (5)) which adds the fast frequency in the variations of the orbital elements, i.e. the planet mean motion n' . In the circular case, the d'Alembert rule implies that $(n'\Lambda' + H) \circ \phi$ only depends on the angles $\lambda' - \omega$ and θ . Consequently, by defining the canonical transformation

$$(15) \quad \begin{array}{ccc} \chi : & \mathcal{M} & \rightarrow \chi(\mathcal{M}) \\ & (\theta, u, x, -i\bar{x}, \lambda', \tilde{\Lambda}') & \mapsto (\theta, u, \zeta, -i\bar{\zeta}, \lambda', \tilde{\Lambda}' - \Gamma) \end{array}$$

with \mathcal{M} , the non-averaged phase space, $\zeta = \sqrt{\Gamma} \exp(i\varphi)$, and $\varphi = \lambda' - \omega$, the Hamiltonian $(n'\Lambda' + H) \circ \phi \circ \chi^{-1}$ becomes autonomous with two degrees of freedom associated with the frequencies ν and $n' - g$. Moreover, this Hamiltonian is related to those in the RF by the pullback by ϕ^{-1} , that is the canonical transformation in Cartesian coordinates. Thus, a trajectory in the RF is generally quasi-periodic with two frequencies. As a consequence, a given trajectory of the RAP generally corresponds to a family of orbits in the RF parametrized by $\varphi(0) \in [0, 2\pi]$ with one more frequency.

For the sake of clarity, we summarize the status of the remarkable orbits in the three different approaches in the table 1.

3.3. Phase portraits of the RAP. The figure 2 displays the phase portraits of the RAP associated with six different values of the parameter e_0 for a Sun-Jupiter like system ($\varepsilon = 0.001$).

In Fig.2a, e_0 is equal to zero: the osculating ellipses of all the orbits are circles. The singular point located at $\theta = u = 0$ corresponds to the collision between the asteroid and the planet, where \overline{H} is not defined (the integral (7) is divergent). The two elliptic fixed points, in $(\theta, u) = (\pm 60^\circ, 0)$, correspond to the Lagrangian configurations L_4 and L_5 whereas the hyperbolic fixed point, close to $(\theta, u) = (180^\circ, 0)$, is associated with the Eulerian configuration L_3 . On the phase portraits described by Nesvorný et al. (2002) two additional equilibria appears: the Eulerian configurations L_1 and L_2 . But as it has

Approach	$e_0 = 0$		$e_0 > 0$			
			$g \neq 0$		$g = 0$	
RAP	FP	PO (ν)	FP	PO (ν)	FP	PO (ν)
\downarrow AP	FP	PO (ν)	$f_{\omega(0)}$ PO (g)	$f_{\omega(0)}$ QPO (ν, g)	$f_{\omega(0)}$ FP	$f_{\omega(0)}$ PO (ν)
\downarrow RF	FP	PO (ν)	$f_{\varphi(0)}$ PO ($n' - g$)	$f_{\varphi(0)}$ QPO ($\nu, n' - g$)	$f_{\varphi(0)}$ PO (n')	$f_{\varphi(0)}$ QPO (ν, n')

TABLE 1. Correspondence between the three approaches for a given trajectory in the RAP. $f_{\omega(0)}, f_{\varphi(0)}$: families parametrized by $\omega(0)$ and $\varphi(0)$ in $[0, 2\pi]$. **FP**: Fixed point. **PO**: Periodic orbit. **QPO**: Quasi-periodic orbit. Parenthesis: associated frequencies.

been shown in Robutel and Pousse (2013), there exists a neighbourhood of the collision singularity inside which the averaged Hamiltonian does not reflect properly the dynamics of the “initial” problem. Indeed, a remainder which depends on the fast variable and that is supposed to be small with respect to $\varepsilon \bar{H}_1$ (see the expressions (4) to (7)) is generated by the averaging process. Although it is the case in the major part of the phase space, when the distance to the collision is of order $\varepsilon^{1/3}$ and less, the remainder is at least of the same order than the perturbation $\varepsilon \bar{H}_1$ (Robutel et al., 2015). Thus, this define an “exclusion zone” inside which the trajectories, and especially the equilibria L_1 and L_2 , fall outside the scope of the averaged Hamiltonian.

The orbits that librate around L_4 or L_5 lying inside the separatrix originating from L_3 correspond to the tadpoles (TP) orbits. For $e_0 = 0$, these two domains form two families of periodic orbits originating in L_4 and L_5 and that are parametrized by $u \geq 0$. We denote them $\mathcal{N}_{L_4}^u$ and $\mathcal{N}_{L_5}^u$. More precisely, they are the Lyapounov families of the Lagrangian equilateral configurations associated with the libration and generally known as the long period families \mathcal{L}_4^l and \mathcal{L}_5^l in the RF (see Meyer and Hall, 1992). Eventually, outside the separatrix lies the horseshoe (HS) domain: the orbits that encompass the three equilibria L_3 , L_4 and L_5 .

If, when $e_0 = 0$, the domain of definition of \bar{H}_{e_0} excludes the origin $\theta = u = 0$, the location of its singularities (associated with the collision) evolves with the parameter e_0 . Indeed, as soon as $e_0 > 0$, the origin becomes a regular point while the set of singular points describes a curve that surrounds the origin. The phase space is now divided in two different domains.

For small e_0 (for example $e_0 = 0.25$ represented in Fig.2b), the domain outside the collision curve has the same topology as for $e_0 = 0$: two stable equilibria close to the L_4 and L_5 ’s location and a separatrix emerging from an hyperbolic fixed point close to L_3 that bounds the TP and the HS domains. However, contrarily to $e_0 = 0$, the fixed points do not correspond to equilibria in the AP and the RF but to periodic orbits. Consequently, orbits

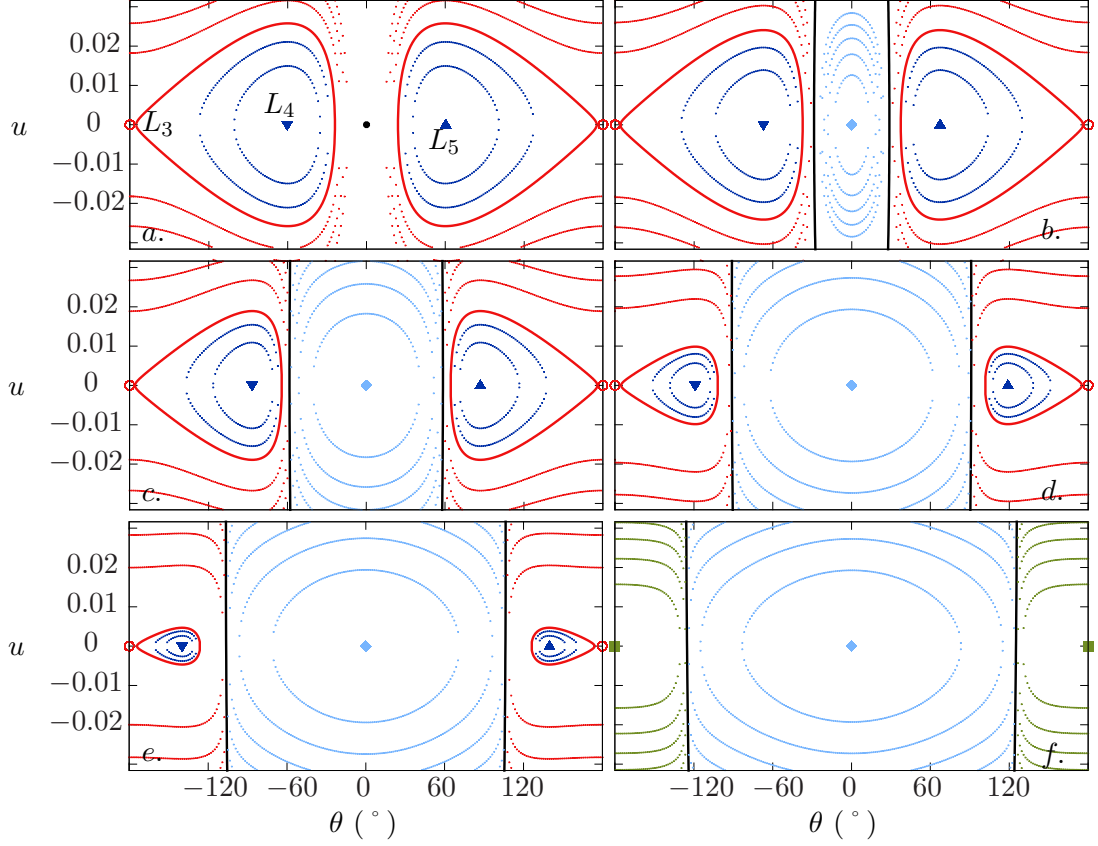


FIGURE 2. Phase portraits of a Sun-Jupiter like system in the circular case. For a, b, c, d, e and f, e_0 is equal to 0, 0.25, 0.5, 0.75, 0.85 and 0.95. The black dot (a.) and curves represent the collision with the planet. The blue, sky blue and red dots are level curves of TP, QS and HS orbits. For $e_0 = 0$, the blue triangles and red circles represent L_4 , L_5 and L_3 , while for $e_0 > 0$ they form the families $\mathcal{G}_{L_4}^{e_0}$, $\mathcal{G}_{L_5}^{e_0}$ and $\mathcal{G}_{L_3}^{e_0}$. From L_3 and the unstable part of $\mathcal{G}_{L_3}^{e_0}$ originates a separatrix that is represented by a red curve. The sky blue diamonds form the family $\mathcal{G}_{QS}^{e_0}$. Eventually the green squares represent the stable part of $\mathcal{G}_{L_3}^{e_0}$ around which trajectories represented by green dots librate.

in their vicinity correspond to quasi-periodic orbits. Thus, by varying e_0 , these fixed points form three one-parameter families that we denote $\mathcal{G}_{L_3}^{e_0}$, $\mathcal{G}_{L_4}^{e_0}$ and $\mathcal{G}_{L_5}^{e_0}$. In the RF, these ones are known as the short period families \mathcal{L}_4^s , \mathcal{L}_5^s and \mathcal{L}_3^s , the Lyapounov families associated with the precession, that emanate from L_4 , L_5 and L_3 (see Meyer and Hall, 1992). Inside

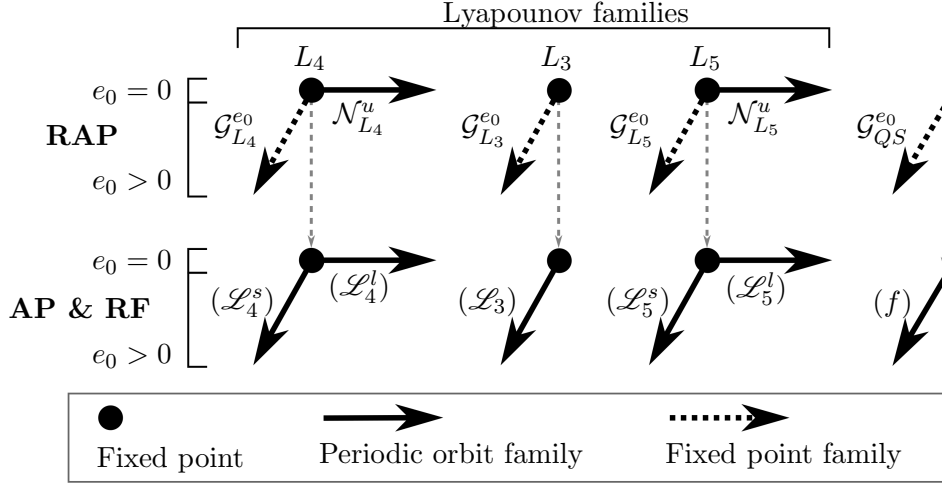


FIGURE 3. Representation of the co-orbital families of periodic orbits from the three different points of view. From each Lagrangian triangular equilibrium originates two Lyapounov families that correspond to a periodic orbit family and a fixed point family in the RAP. These families are associated with the long and short period families in the AP and the RF. L_3 being a saddle center type in the RAP, only one Lyapounov family emanates from this equilibrium that is a fixed point family in the RAP and a periodic orbit family in the AP and RF. Eventually, for $e_0 > 0$, there exists a family of fixed points in the RAP that is not a Lyapounov family: $\mathcal{G}_{QS}^{e_0}$. This family is associated with a periodic orbit family in the RF: the family f .

the collision curve appears a new domain containing orbits that librate around a fixed point of coordinates close to the origin: the QS domain. By varying e_0 , the fixed points form a one-parameter family that originates from the singular point for $e_0 = 0$. We denote it $\mathcal{G}_{QS}^{e_0}$. In the RF, these fixed points correspond to a family of periodic orbits with a frequency $n' - g$ and such that $\theta = 0^\circ$. Hence, $\mathcal{G}_{QS}^{e_0}$ is related to the family f .

Thus for small eccentricities, TP, HS and QS domains are structured around two periodic orbit families and four fixed point families that we outline in Fig.3 to clarify their representations in the different approaches.

For higher values of e_0 (cf. Fig.2c, d, e and f), the topology of the phase portraits does not change inside the collision curve: the QS domain is always present, but its size increases until it dominates the phase portrait for high eccentricity values. Outside the collision curve, the situation is different. As e_0 increases, the two stable equilibria get closer to the hyperbolic fixed point, which implies that the TP domains shrink and vanish when the three merge. This bifurcation generates a new domain inside which orbits that librate around the fixed point close to $(\theta, u) = (180^\circ, 0)$ (cf. Fig.2f). A similar result was found

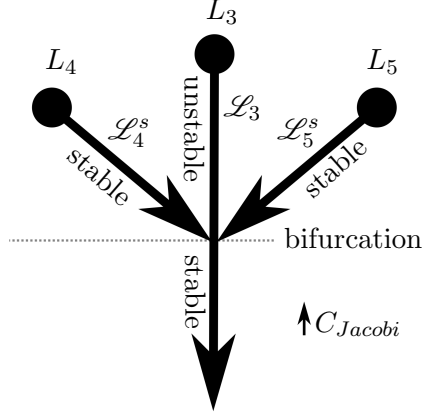


FIGURE 4. Representation of the result of Deprit et al. (1967) in the RF: the merge of the short period families \mathcal{L}_4^s and \mathcal{L}_5^s with \mathcal{L}_3 and bifurcation of the latter that becomes stable.

by Deprit et al. (1967) for an Earth-Moon like system in the circular case ($\varepsilon = 1/81$). In the RF, the authors showed that the short period families \mathcal{L}_4^s and \mathcal{L}_5^s terminate on a periodic orbit of \mathcal{L}_3 (see the outline in Fig.4).

Now, let us focus on the QS domain. As mentioned above, there exists an exclusion zone in the vicinity of the collision curve such that the QS orbits does not represent “real” trajectories of the initial problem. For high eccentricities, the QS dominates the phase portraits; the size of the intersection between the QS domain and the exclusion zone is small relatively to the whole domain. However by decreasing e_0 , the QS domain shrinks with the collision curve. As a consequence, the relative size of the intersection increases until a critical value of e_0 where the exclusion zone contains all the QS orbits. In this case, the AP and a fortiori the RAP are not relevant to study the QS motion.

A simple way to estimate a validity limit of these two approaches is to consider that the whole QS domain is excluded if and only if $\mathcal{G}_{QS}^{e_0}$ is inside the exclusion zone. Thus the study of the fixed points family $\mathcal{G}_{QS}^{e_0}$ allows to determinate the eccentricity value under which the averaging method cannot be applied to QS motion. This method is implemented in the following section.

3.4. Fixed point families of the RAP. The stability of the fixed point belonging to the $\mathcal{G}_{QS}^{e_0}$ family is deduced from the eigenvalues of the Hessian matrix of \overline{H}_{e_0} . When the fixed point is elliptic, its eigenvalues are equal to $\pm i\nu$, where the real number ν is the rotation frequency around the equilibrium. Moreover, the precession frequency of the corresponding orbit is given by $g = -\frac{\partial}{\partial \Gamma} \overline{H}_{e_0}$.

The evolution of the location and of the frequencies of the orbits associated with the families $\mathcal{G}_{QS}^{e_0}$, $\mathcal{G}_{L_3}^{e_0}$, $\mathcal{G}_{L_4}^{e_0}$ and $\mathcal{G}_{L_5}^{e_0}$ versus e_0 are described in Fig.5 for a mass ratio equal to $\varepsilon = 10^{-3}$ (a Sun-Jupiter like system).

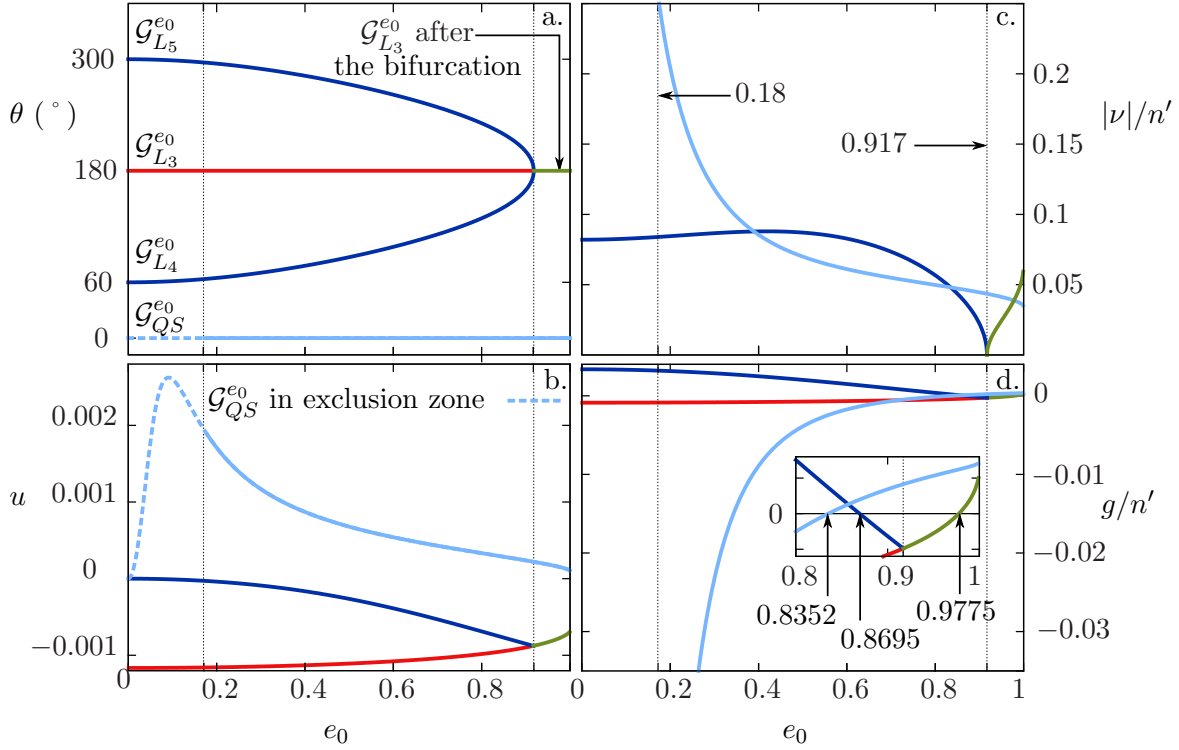


FIGURE 5. Location in θ (a.) and u (b.) and frequencies $|\nu|$ (c.) and g (d.) of the fixed points families for a Sun-Jupiter like system ($\varepsilon = 10^{-3}$). \mathcal{F}_{L_4} and \mathcal{F}_{L_5} (blue curves) merge with $\mathcal{G}_{L_3}^{e_0}$ (red curve) which gives rise to a stable family of fixed points (green curve). The AP is relevant for QS motion when $\mathcal{G}_{QS}^{e_0}$ (sky blue curve) is a continuous curve. There are particular orbits without precession on each family which correspond to degenerated fixed points of the AP.

The red curve close to $(\theta, u) = (180^\circ, 0)$ represents the family $\mathcal{G}_{L_3}^{e_0}$ while the two blue curves that start in L_4 and L_5 correspond to $\mathcal{G}_{L_4}^{e_0}$ and $\mathcal{G}_{L_5}^{e_0}$. As described in section 3.3, by increasing e_0 these two last families merge with $\mathcal{G}_{L_3}^{e_0}$ for $e_0 \simeq 0.917$ (vertical dashed line). Above this critical value, the last family becomes stable (green curves in Fig.5).

The sky blue curve located nearby $(\theta, u) = (0^\circ, 0)$ represents the family $\mathcal{G}_{QS}^{e_0}$. Along this family, for $0.4 \leq e_0 < 1$, the frequencies $|\nu|$ and $|g|$ are of the same order as those of the TP equilibria, but the sign of g is different. Then, by decreasing e_0 , the moduli of the frequencies increase and tend to infinity. When the frequencies reach values of the same order or higher than the fast frequency, $\mathcal{G}_{QS}^{e_0}$ enters the exclusion zone and the averaged problem does not describe accurately the quasi-satellite's motions.

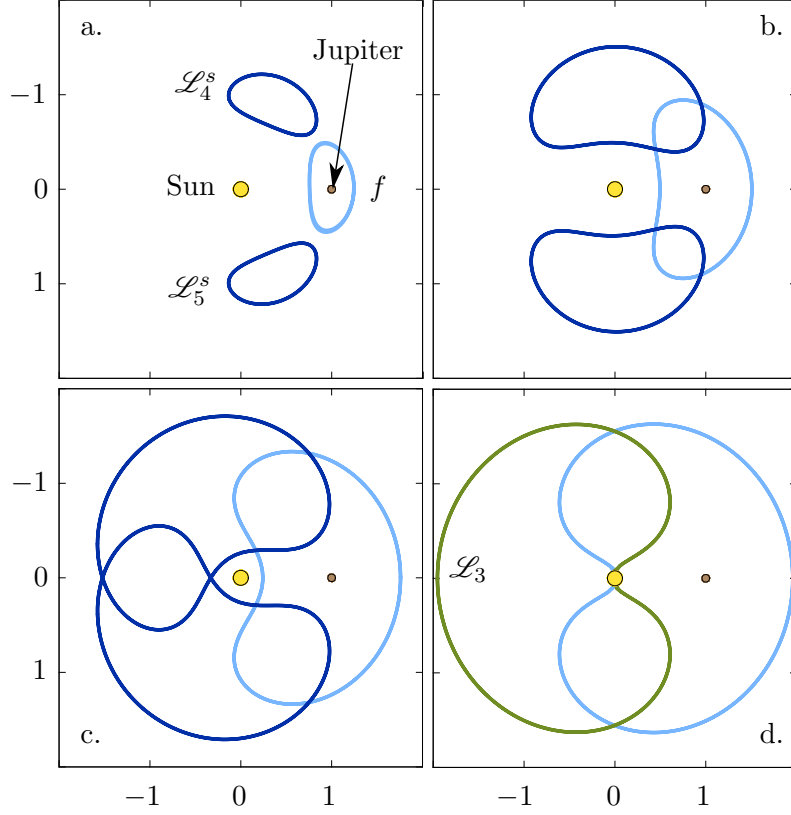


FIGURE 6. Periodic orbits in the rotating frame associated with stable orbits of $\mathcal{G}_{L_4}^{e_0}$, $\mathcal{G}_{L_5}^{e_0}$, $\mathcal{G}_{L_3}^{e_0}$ and $\mathcal{G}_{QS}^{e_0}$ for $e_0 = 0.25$ (a.), 0.5 (b.), 0.75 (c.) and 0.95 (d.) (see Fig.2 b, c, d and f). The blue curves are associated with \mathcal{L}_4^s ; the sky blue curve with the family f and the green curve corresponds to \mathcal{L}_3 after the bifurcation.

In order to estimate an eccentricity range where the averaged problem is adapted to QS motion, we consider that $\mathcal{G}_{QS}^{e_0}$ is outside the exclusion zone when $|g|$ and $|\nu|$ are lower than $n'/4$. Fig.5 shows that this quantity is given by $e_0 = 0.18$ (vertical dashed line). Therefore, the AP and RAP are relevant to study $\mathcal{G}_{QS}^{e_0}$ and thus the QS motion for $e_0 \geq 0.18$ in the Sun-Jupiter system.

Now, we focus on the variations of g along each families of fixed points. For each of them, the frequency is monotonous and crosses zero for a critical value of eccentricity: $e_0 \simeq 0.8352$ for $\mathcal{G}_{QS}^{e_0}$, $e_0 \simeq 0.8695$ for $\mathcal{G}_{L_4}^{e_0}$ and $\mathcal{G}_{L_5}^{e_0}$, and $e_0 \simeq 0.9775$ for $\mathcal{G}_{L_3}^{e_0}$. According to the section 3.2, these particular trajectories in the RAP correspond to circles of fixed points in the AP, and periodic orbits of frequency n' in the RF, that is frozen ellipses in the heliocentric frame. We denote them G_{QS} , G_{L_4} , G_{L_5} and G_{L_3} .

To conclude this section, we connect the fixed points families in the RAP to the corresponding trajectory in the RF. Outside the exclusion zone, the transformation of these ones by $\phi \circ \chi \circ \mathcal{C} \circ \psi_{e_0}^{-1}$ provides us a first order approximation of their initial conditions in the RF. Therefore, by improving them with an iterative algorithm that removes the frequency ν (Couetdic et al., 2010), we integrated the corresponding trajectories in the RF. An example of stable trajectories is represented on the figure 6 for several values of e_0 .

For a Sun-Jupiter like system, the families $\mathcal{G}_{L_4}^{e_0}$, $\mathcal{G}_{L_5}^{e_0}$ provide the entire short period families, from their respective equilibrium to their merge with $\mathcal{G}_{L_3}^{e_0}$ and its collision orbit with the Sun. On the contrary, $\mathcal{G}_{QS}^{e_0}$ provide only a part of the family f , from the collision with the Sun to the orbit with $e_0 = 0.18$.

The figure 6 shows that by increasing e_0 , the size of the periodic trajectories in the RF increases. As expected, the libration center of the family f is located close to the planet, while those of \mathcal{L}_4^s and \mathcal{L}_5^s shift from L_4 and L_5 towards L_3 where they merge with those of \mathcal{L}_3 . After the bifurcation, only trajectories of the f and \mathcal{L}_3 families remain.

4. QUASI-SATELLITE'S DOMAINS IN THE ROTATING FRAME WITH THE PLANET

4.1. The family f in the RF. The RAP seems to be the most adapted approach to understand the co-orbital motion in the circular case. However, the averaged approaches have the drawback to be poorly significant in the exclusion zone that surround the singularity. For the QS motion, we showed in the section 3 that the whole domain could not be reachable by low eccentric orbits, that is when the trajectories get closer to the planet. As a consequence, to understand the QS nearby the planet and connect our results in the averaged approaches, we chose to revisit the classical works (Henon and Guyot, 1970; Benest, 1975) on the family f in the RF.

In the RF with the planet on a circular orbit, the problem has two degrees of freedom that we represent by the position $\mathbf{r} = (\xi, \eta)$ and the velocity $\dot{\mathbf{r}} = (\dot{\xi}, \dot{\eta})$ in the frame whose origin is the planet position, the horizontal axis is the Sun-planet alignment and the vertical axis, its perpendicular (see Fig.7).

In the neighbourhood of the family f , each trajectory crosses the axes $\{\eta = 0\}$ with $\dot{\eta} < 0$ when $\xi > 0$. By defining the Poincaré map Π_T associated with this section, the problem could be reduced to one degree of freedom represented by $(\xi, \dot{\xi})$, T being the time between two consecutive crossings. Thus, in this Poincaré section a periodic orbit of the family f corresponds to a fixed point whose coordinates in the RF are $(\xi, 0, 0, \dot{\eta})$ with $T = 2\pi/(n' - g)$. The stability of the periodic orbit is deduced from the trace of the monodromy matrix $d\Pi_T$ evaluated at the fixed point. Moreover, when the fixed point is stable, the libration frequency ν is obtained from its two conjugated eigenvalues $(\kappa, \bar{\kappa})$ such as $\kappa = \exp i\nu T$.

4.2. Application to a Sun-Jupiter like system. The figure 8 and 9a represent the family f in the $(\xi, \dot{\eta})$ plane (red curve) and its reachable part in the averaged approaches (sky blue curve).

Fig.8 shows that the family f extends from the orbits in an infinitesimal neighbourhood of the planet to the collision orbit with the Sun. Although, the whole family is linearly

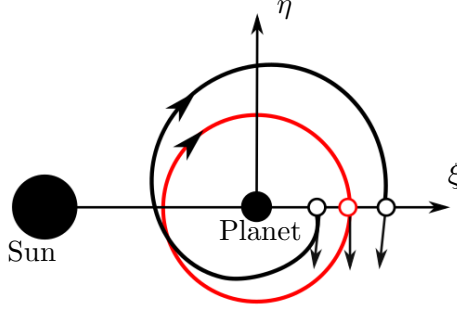


FIGURE 7. Representation of retrograde satellite trajectories in the RF. Red curve: periodic trajectory of the family f . Black curve: trajectory in the neighbourhood of the family f that intersects the Poincaré section (black circles).

stable, we cannot predict the size of the stable region surrounding it. Indeed, resonances with its normal frequencies could reduced this region. This is what occurs in two points of the family f (blue crosses and dashed lines) where the stability domain's diameter tends to zero. Consequently, these two periodic orbits divide the neighbourhood of the family f in three connected domains that we outlined in grey in Fig.8 and Fig.9a.

The figure 9b exhibits the variations of the frequencies ν and $n' - g$ along the family. Comparing to Fig.5b, we remark that ν/n' does not tend to infinity when the periodic orbits get closer to the planet, but increases and tends to 1. Likewise, Fig.9b highlights that the resonance between the frequencies of the system is $\nu/(n' - g) = 1/3$ and that the three domains are neatly defined in terms of frequencies as follows:

$$(16) \quad \text{RS} : \begin{cases} 3\nu < n' - g \\ |g| > n' \end{cases}, \quad \text{QS}_b : \quad 3\nu > n' - g$$

$$\text{and} \quad \text{QS}_h : \begin{cases} 3\nu < n' - g \\ |g| < n' \end{cases}.$$

The upper bound of the closest domain to the planet being the L_2 position, that is the limit of the Hill's sphere, then this one corresponds to the “satellized” retrograde satellite (RS) orbits. This domain consists of trajectories dominated by the gravitational influence of the planet whereas the star acts as a perturbator. Thus the planetocentric osculating ellipses are the most relevant variables to represent the motion and perturbative treatments are possible. The domain outside the Hill's sphere corresponds to the QS that is divided in two others domains.

The domain of QS_h orbits, that is the heliocentric QS, corresponds to the farthest domain to the planet, which implies that this body acts as a perturbator whereas the influence of the star dominates the dynamics. Therefore, the heliocentric orbital elements

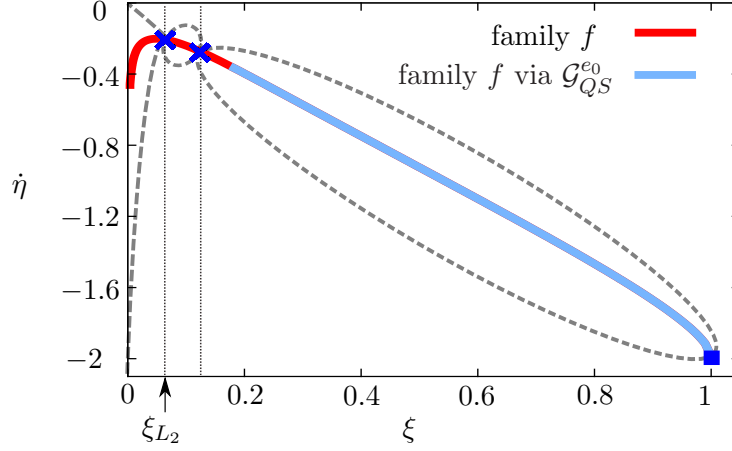


FIGURE 8. The family f in the $(\xi, \dot{\eta})$ plane (red curve) and its reachable part in the AP via \mathcal{G}_{QS}^{e0} (sky blue curve). The two blue crosses indicate the resonant orbits (1 : 3) that split the domain. The blue square indicates the collision orbit with the Sun. The grey outline schematizes the three connected domains of the family f neighbourhood.

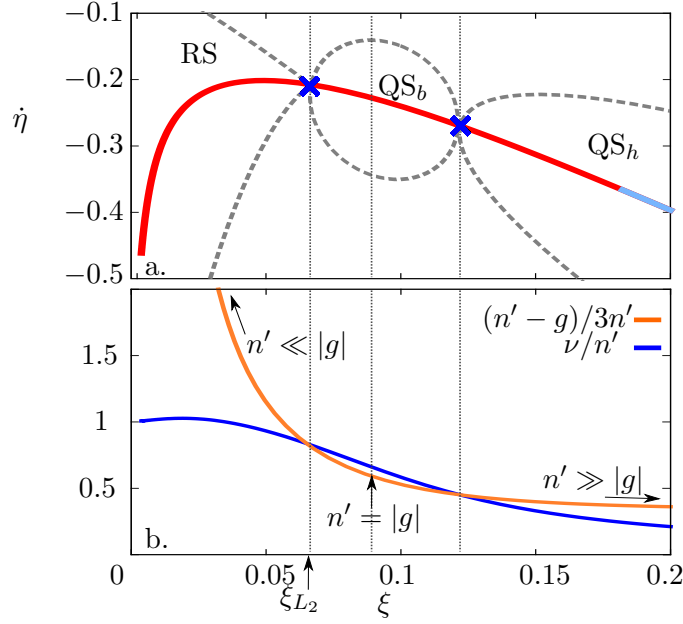


FIGURE 9. (a.) Zoom in of Fig.8 on the two periodic orbits in 1 : 3 resonance. (b.) Variation of the frequencies of the system along the family f . Comparing to Fig.5b, ν/n' does not tend to infinity when the periodic orbits get closer to the planet, but increases and tends to 1. The 1 : 3 resonance splits the neighbourhood in three domains neatly defined in terms of frequencies: retrograde satellite (RS), binary quasi-satellite (QS_b) and heliocentric quasi-satellite (QS_h)

are well suited to the problem, and the perturbative treatment as well as the averaging over the fast angle are natural. As a consequence, it is the QS_h trajectories that are reachable in the averaged problem. As the orbits of the family f included in the QS_h domain cross the Poincaré section at their aphelion, the ξ coordinates is related to e_0 by the expression $\xi = e = e_0 + \mathcal{O}(\varepsilon)$.

The third domain, that we called the binary QS domain (QS_b), is intermediate between the RS and QS_h ones. In this region, none of the two massive bodies has a dominant influence on the massless one. As a consequence, the frequencies n' and g could be of the same order or even equal, making inappropriate any method of averaging.

Remark that in the planetary problem, Hadjidemetriou and Voyatzis (2011) highlight a family of periodic orbits that corresponds to the family f . Indeed, along this family that ranges from orbits for which the two planets collide with the star to the orbits where the two planets are mutually satellized, all trajectories are stable and satisfy $\theta = 0^\circ$. These authors also decomposed the family in three domains, denoted A , B and planetary, which seem to correspond to our RS, QS_b and QS_h domains.

4.3. Extension to arbitrary masses. By varying the mass ratio ε , we follow the evolution of the boundaries of the three domains along the family f as well as the validity limit of the averaged problem. In Fig.10, the parameter ε ranges from 10^{-7} to 0.0477 which is the critical mass ratio where a part of the family f becomes unstable (see Henon and Guyot, 1970). For Sun-terrestrial planet systems, the size of the QS_b and RS domains is negligible with respect to the QS_h one. As a consequence, for these systems, the AP and RAP are fully adapted to describe the main part of the family f and its neighbourhood (except for very small eccentricities). For Sun-giant planet systems as well as the Earth-Moon system, the gravitational influence of the planet being stronger, the size of the QS_b domain f increases until to be of the same order than those of the RS one while the size of the QS_h decreases. As $e_0 = \xi + \mathcal{O}(\varepsilon)$, we established that for the Sun-Uranus, Sun-Saturn, Sun-Jupiter and Earth-Moon systems, the QS_h orbits are reachable in the averaged problem by e_0 greater than 0.08, 0.13, 0.18 and 0.5. Then, by increasing ε , the QS_b domain becomes dominant while the QS_h one is reduced so much that the averaged problem becomes useless for all values of e_0 ($\varepsilon \simeq 0.04$). Consequently, for the Pluto-Charon system ($\varepsilon \simeq 1/10$) none QS_h trajectory could be described in the averaged approaches. Moreover, according to the stability map of the family f in Benest (1975), this system could not harbour a QS_h companion: only QS_b and RS trajectories exist for this value of mass ratio.

5. ON THE FROZEN ORBITS: AN EXTENSION TO THE ECCENTRIC CASE ($e' > 0$)

An important result of our study in the circular case has been to highlight the particular orbits G_{QS} , G_{L_3} , G_{L_4} and G_{L_5} , circles of fixed points in the averaged problem that correspond to frozen ellipses in the heliocentric frame (see the section 3.4). A natural question is to know if these structures are preserved when a small eccentricity is given to the planetary orbit. This question can be addressed in a perturbative way. Indeed, for sufficiently low values of planet's eccentricity, the Hamiltonian of the problem reads $\overline{H}' = \overline{H} + e'R$, i.e. the perturbation of the Hamiltonian in the circular case by the first order term in planetary

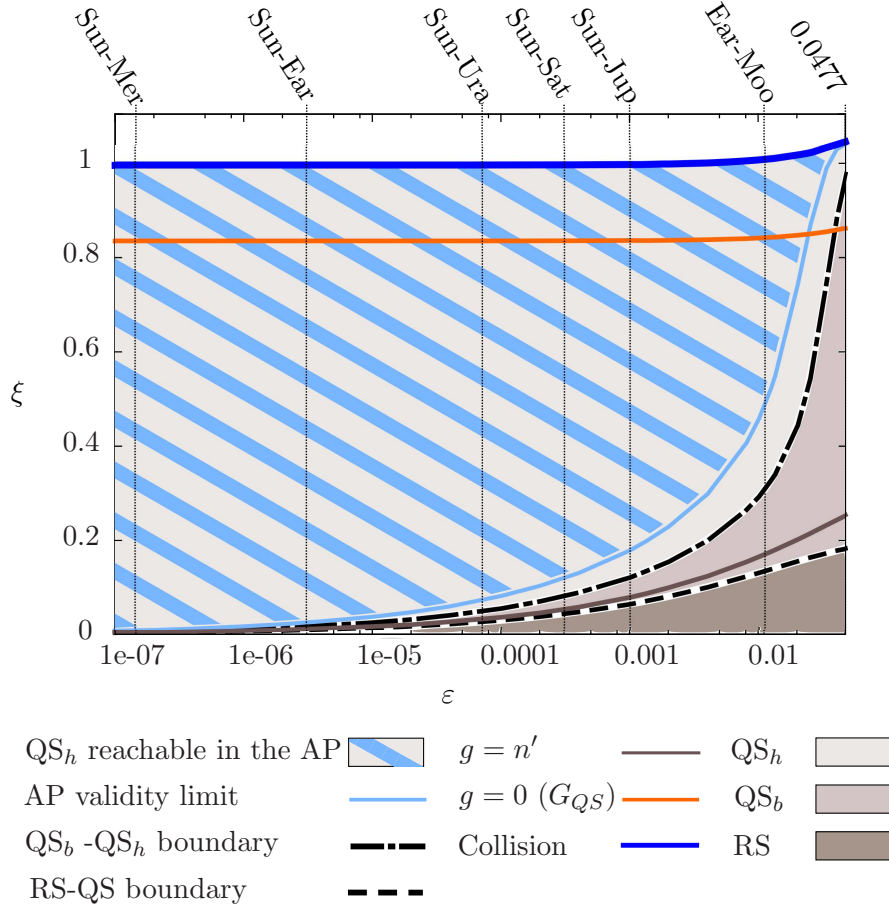


FIGURE 10. Evolution of the RS, QS_b and QS_h boundaries along the family f by varying the mass ratio ε . For small ε , the QS_h domain dominates the family f implying that the AP and the RAP are fully adapted to study the QS motion. By increasing ε , the size of the part associated with the RS and the QS_b trajectories increases making not reachable the orbits with small eccentricities in the averaged problem. Eventually, for $\varepsilon > 0.01$, the RS and the QS_b domains becomes dominant while the QS_h one is reduced so much that the averaged problem becomes useless for all values of e_0 .

eccentricity. However, as ω is no longer an ignorable variable in this Hamiltonian, the dimension of the phase space could not been reduced as in the section 3 and the persistence of fixed points is not necessary guaranteed.

In the present paper, we limit our approach to numerical explorations of the phase space. For a very low value of e' in a Sun-Jupiter like system, numerical simulations show

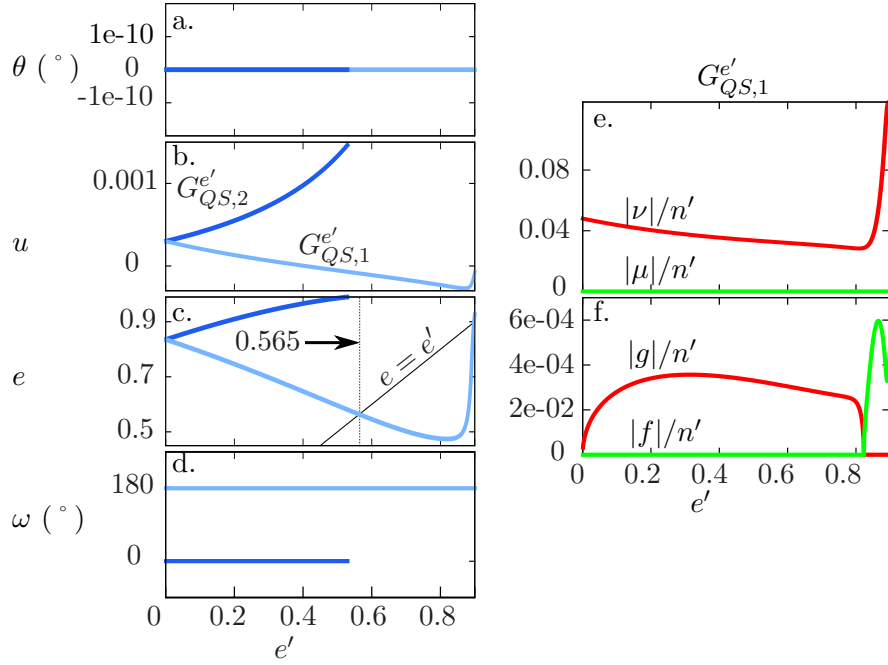


FIGURE 11. a,b,c and d: orbital elements of the families of fixed points $G_{QS,2}^{e'}$ and $G_{QS,1}^{e'}$ versus e' . f and g: variations of the moduli of the real and imaginary part of the eigenvalues of the Hessian matrix along $G_{QS,1}^{e'}$. $G_{QS,1}^{e'}$ is a stable family until $e' < 0.8$ with $\theta = 0^\circ$ and configuration of anti-aligned ellipses. Moreover, this family possesses a particular orbit where $e = e' \simeq 0.565$. On the contrary, $G_{QS,2}^{e'}$ is unstable with $\theta = 0^\circ$ and a configuration of aligned ellipses.

that although each circle of fixed points is destroyed, two fixed points survived to the perturbation. One is stable and the other unstable. We denote these fixed points $G_{X,1}^{e'}$ and $G_{X,2}^{e'}$ with X corresponding to QS, L_4 , L_5 and L_3 . By varying e' , we followed them show families of equilibria that originate from the circles of fixed points. For all these fixed points, the associate linear differential system processes two couples of eigenvalues comprised of $\pm\mu$ or $\pm i\nu$ and $\pm f$ or $\pm ig$ where μ , f , ν and g are real, whether the equilibrium is stable or unstable. If these eigenvalues are all imaginary then they characterized an elliptic fixed point with libration and secular precession frequencies ν and g . Otherwise, the fixed point is unstable. Thus, we also characterized the stability of the family by varying e' . Their initial conditions and the moduli of the real and imaginary part of the eigenvalues versus e' are plotted on Fig.11, 12 and 13.

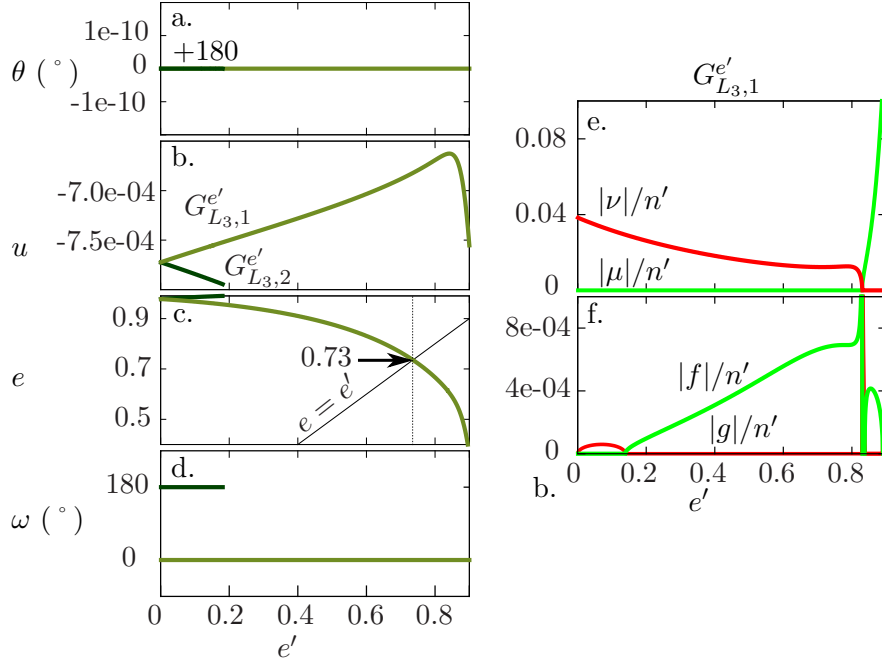


FIGURE 12. a,b,c and d: orbital elements of the families of fixed points $G_{L3,2}^{e'}$ and $G_{L3,1}^{e'}$ versus e' . f and g: variations of the moduli of the real and imaginary part of the eigenvalues of the Hessian matrix along $G_{L3,1}^{e'}$. $G_{L3,1}^{e'}$ is stable for $e' \leq 0.15$ with $\theta = 180^\circ$ and a configuration of aligned ellipses. Moreover, this family possesses a particular orbit with $e' = e \simeq 0.73$ where the secondary and the particle share the same ellipses. On the contrary, $G_{L3,2}^{e'}$ is unstable with $\theta = 180^\circ$ and a configuration of anti-aligned ellipses.

According to the figures 11, 12 and 13, we find eight families of fixed points in the averaged problem that correspond to frozen ellipses in the heliocentric frame. However, among them, two are more relevant: $G_{QS,1}^{e'}$ and $G_{L3,1}^{e'}$.

The family $G_{QS,1}^{e'}$, that originates from G_{QS} , is stable until $e' \simeq 0.8$. It corresponds to a configuration of two ellipses in anti-alignment with $\theta = 0^\circ$ and a very high eccentricity that decreases when e' increases (the slope being close to $\frac{de}{de'} = -1/2$). On the contrary, the family $G_{L3,1}^{e'}$ originates from $G_{L3}^{e_0}$ and is only stable for $e' \in [0, 0.15]$. It describes a configuration with ellipses in alignment, $\theta = 180^\circ$ and a very high eccentricity that decreases when e' increases. Along these two families, there exists a critical value of e' where the planet and the asteroid ellipses have the same eccentricities. The dashed lines of the figures 11 and 12 show that these particular orbits exist for $e' = e \simeq 0.565$ along $G_{QS,1}^{e'}$ and $e' = e \simeq 0.73$ along $G_{L3,1}^{e'}$.

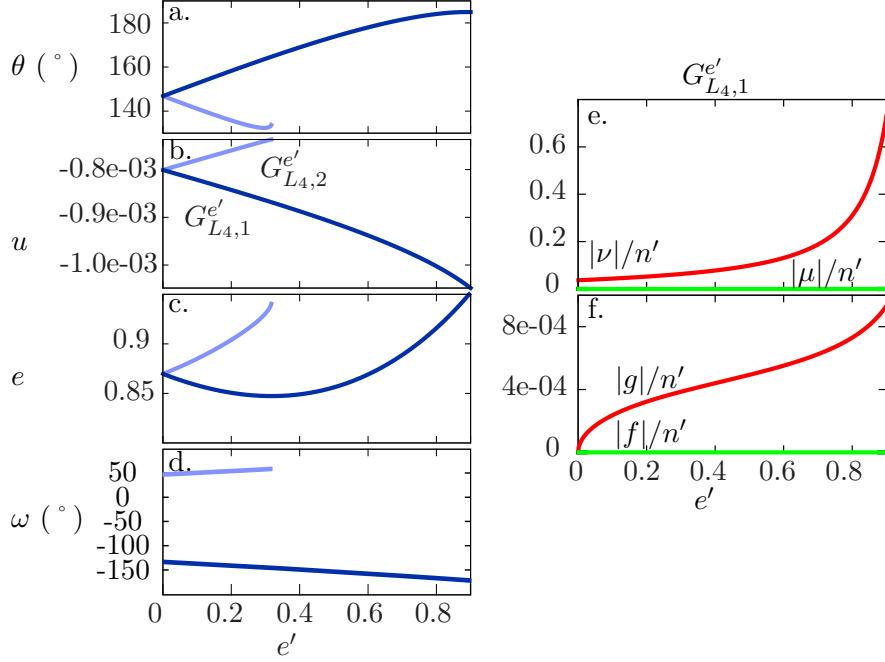


FIGURE 13. a,b,c and d: orbital elements of the families of fixed points $G_{L4,2}^{e'}$ and $G_{L4,1}^{e'}$ versus e' . e and f: variations of the moduli of the real and imaginary part of the eigenvalues of the Hessian matrix along $G_{L4,1}^{e'}$. The whole family $G_{L4,1}^{e'}$ is stable whereas $G_{L4,2}^{e'}$ is unstable.

Let us notice that these two families have been highlighted in the planetary problem. Indeed, these two families have certainly to do with the stable and unstable families of periodic orbits described in Hadjidemetriou et al. (2009) and Hadjidemetriou and Voyatzis (2011). As regard $G_{QS,1}^{e'}$, it could also be associated with the QS fixed point family in Giuppone et al. (2010). In Giuppone et al. (2010) as well as in Hadjidemetriou and Voyatzis (2011), these authors remarked that the configuration described by $G_{QS,1}^{e'}$ with two equal eccentricities exists with an eccentricity value close to 0.565 for several planetary mass ratio. In our study, we establish that this particular orbit also exists in the RTBP for $e = e' \simeq 0.565$ (see Fig.11). Likewise, according to Hadjidemetriou et al. (2009), the configuration described by $G_{L3,1}^{e'}$ with two equal eccentricities seems to exist in the planetary problem for an eccentricity value close to 0.73. Consequently, this suggests that these two particular configurations are weakly dependent on the ratio of the planetary masses.

Eventually, we remark that the existence of some of these eight configurations has already been showed. Indeed, in the range $0.01 \leq e' \leq 0.5$, Nesvorný et al. (2002) exhibit QS stable and unstable fixed points. Likewise, Bien (1978) and Edelman (1985) highlighted some frozen ellipses in co-orbital motion in the Sun-Jupiter system with $e' = e'_{Jupiter} \simeq 0.048$.

The first author found six high eccentric fixed points denoted $P_1, Q_1, P_2, Q_2, P_3, Q_3$ that correspond to $G_{L_4,1}^{e'}$, $G_{L_4,2}^{e'}$, $G_{L_5,1}^{e'}$, $G_{L_5,2}^{e'}$, $G_{QS,1}^{e'}$ and $G_{QS,2}^{e'}$. The other found a frozen ellipse in co-orbital resonance with $e = 0.975$ and $\theta = 180^\circ$, that is an orbit of $G_{L_3,1}^{e'}$.

6. CONCLUSIONS

In this paper, we clarify the definition of quasi-satellite motion and estimate a validity limit of the averaged approach by revisiting the planar and circular Restricted Three-Body Problem.

First of all, we focussed on the co-orbital resonance via the averaged problem and showed that the study of the phase portraits of the reduced averaged problem parametrized by e_0 allow to understand its global dynamics. Indeed, they reveal that tadpole, horseshoe and quasi-satellite domains are structured around four families of fixed points originating from L_4, L_5 ($\mathcal{G}_{L_4}^{e_0}$ and $\mathcal{G}_{L_5}^{e_0}$), L_3 ($\mathcal{G}_{L_3}^{e_0}$) and the singularity point for $e_0 = 0$ ($\mathcal{G}_{QS}^{e_0}$). By increasing e_0 , the quasi-satellite orbits appear inside the domain opened by the collision curve for $e_0 > 0$ and becomes dominant for high eccentricities. On the contrary, tadpole and horseshoe domains shrink and vanish when $\mathcal{G}_{L_4}^{e_0}$ and $\mathcal{G}_{L_5}^{e_0}$ get closer and merge $\mathcal{G}_{L_3}^{e_0}$. Moreover, we showed that this remaining family bifurcates and generates a new domain of high eccentric orbits librating around $(\theta, u) = (180^\circ, 0)$.

However, the averaged approaches having the drawback to be poorly significant in the exclusion zone, we highlighted that for sufficiently small eccentricities, the whole quasi-satellite domain is contained inside it which makes this type of motion not reachable by averaging process. The study of the evolution of the libration and secular precession frequencies along $\mathcal{G}_{QS}^{e_0}$, allowed us to show that the family f and a fortiori the quasi-satellite domain are not reachable by $e_0 < 0.18$ in a Sun-Jupiter like system.

In order to clarify the terminology to use between “retrograde satellite” or “quasi-satellite” when these orbits are close encountering trajectories with the planet, we revisited the works on the family f in the rotating frame. We highlighted that the family f possesses two particular orbits that divide its neighbourhood in three connected areas: the retrograde satellite, binary quasi-satellite and heliocentric quasi-satellite domains. We established that the last one is the only one reachable in the averaged approaches.

The study of the frequencies of the fixed point families of the reduced averaged problem has also shown some frozen orbits in the heliocentric frame which are equivalent to circles of fixed points in the averaged problem. In order to exhibit fixed points when the planet’s orbit is eccentric, we highlighted numerically that from each circles of fixed points originates at least two families of fixed points parametrized by the planet eccentricity. Among them, $G_{QS,1}^{e'}$ is the most interesting as it is in quasi-satellite motion with a configuration of two anti-aligned ellipses and connected to the stable family described in Hadjidemetriou et al. (2009) in the planetary problem. Moreover, $G_{QS,1}^{e'}$ as well as the family in the planetary problem possess a configuration with equal eccentricities for an eccentricity value close to 0.565. As a consequence, this suggests that this remarkable configuration is weakly dependent to the ratio between the planetary masses. Likewise, let us mentioned that this configuration is similar to those of the family “A.1/1” described in Broucke (1975) in the

general Three-Body Problem with three equal masses which suggests a connection between them.

When $e_0 > 0.4$, we denoted that the moduli of the libration frequency ν and of the secular precession frequency g along the family f are of the same order than those of the two tadpole periodic orbit families. Thus, in the framework of long-term dynamics of the Jovian quasi-satellite asteroids in the solar system, we can assume that a study of the global dynamics by means of the frequency map analysis will reveal resonant structures close to those of the trojans identified in Robutel and Gabern (2006). However, by remarking that the direction of the perihelion precession being the opposite of those of the planets in the solar system, resonances with these secular frequencies should be of higher order in comparison to the tadpoles orbits. On the contrary, resonances with their node precession should be of lower order. These questions will be addressed in a forthcoming work

NOMENCLATURE

L_1, L_2, L_3 Eulerian configurations
 L_4, L_5 Lagranian equilateral configurations
 $\mathcal{G}_{L_3}^{e_0}, \mathcal{G}_{L_4}^{e_0}, \mathcal{G}_{L_5}^{e_0}$ Fixed point families that originate from L_3, L_4 and L_5 in the RAP
 $\mathcal{G}_{QS}^{e_0}$ Fixed point family associated with the QS in the RAP
 $G_{L_3}, G_{L_4}, G_{L_5}, G_{QS}$ Particular orbits of $\mathcal{G}_{L_3}^{e_0}, \mathcal{G}_{L_4}^{e_0}, \mathcal{G}_{L_5}^{e_0}$ and $\mathcal{G}_{QS}^{e_0}$ with $g = 0$. Fixed points in the AP
 $G_{L_3,1}^{e'}, G_{L_3,2}^{e'}, G_{L_4,1}^{e'}, G_{L_4,2}^{e'}, G_{L_5,1}^{e'}, G_{L_5,2}^{e'}, G_{QS,1}^{e'}, G_{QS,2}^{e'}$ Families of fixed points in the AP with $e' > 0$ that originate from $G_{L_3}, G_{L_4}, G_{L_5}, G_{QS}$
 $\mathcal{L}_4^s, \mathcal{L}_5^s$ Short period families that originate from L_4 and L_5 in the RF
 $\mathcal{L}_3^l, \mathcal{L}_4^l, \mathcal{L}_5^l$ Long period families that originate from L_3, L_4 and L_5 in the RF
 $\mathcal{N}_{L_4}^u, \mathcal{N}_{L_5}^u$ Periodic orbit families that originate from L_4 and L_5 in the RAP
 f Periodic orbit family associated with the RS and QS in the RF
 QS_b Binary Quasi-satellite
 QS_h Heliocentric Quasi-satellite
AP Averaged Problem
HS Horseshoe
QS Quasi-satellite
RAP Reduced Averaged Problem
RF Rotating Frame with the planet
RS Retrograde-satellite
RTBP Restricted Three-Body Problem
TBP Three-Body Problem
TP Tadpole

REFERENCES

Beaugé, C. and Roig, F. (2001). A Semianalytical Model for the Motion of the Trojan Asteroids: Proper Elements and Families. *Icarus*, 153:391–415.

- Benest, D. (1974). Effects of the Mass Ratio on the Existence of Retrograde Satellites in the Circular Plane Restricted Problem. *Astronomy & Astrophysics*, 32:39.
- Benest, D. (1975). Effects of the mass ratio on the existence of retrograde satellites in the circular plane restricted problem. II. *Astronomy & Astrophysics*, 45:353–363.
- Benest, D. (1976). Effects of the mass ratio on the existence of retrograde satellites in the circular plane restricted problem. III. *Astronomy & Astrophysics*, 53:231–236.
- Bien, R. (1978). Long-period effects in the motion of Trojan asteroids and of fictitious objects at the 1/1 resonance. *Astronomy and Astrophysics*, 68:295–301.
- Brasser, R., Innanen, K., Connors, M., Veillet, C., Wiegert, P. A., Mikkola, S., and Chodas, P. (2004). Transient co-orbital asteroids. *Icarus*, 171(1):102–109.
- Broucke, R. (1975). On relative periodic solutions of the planar general three-body problem. *Celestial Mechanics*, 12:439–462.
- Broucke, R. A. (1968). Periodic orbits in the restricted three-body problem with earth-moon masses.
- Connors, M., Chodas, P., Mikkola, S., Wiegert, P. A., Veillet, C., and Innanen, K. (2002). Discovery of an asteroid and quasi-satellite in an Earth-like horseshoe orbit. *Meteoritics & Planetary Science*, 37(10):1435–1441.
- Connors, M., Veillet, C., Brasser, R., Wiegert, P. A., Chodas, P., Mikkola, S., and Innanen, K. (2004). Discovery of Earth’s quasi-satellite. *Meteoritics & Planetary Science*, 39(8):1251–1255.
- Couetdic, J., Laskar, J., Correia, A. C. M., Mayor, M., and Udry, S. (2010). Dynamical stability analysis of the HD 202206 system and constraints to the planetary orbits. *Astronomy and Astrophysics*, 519:A10.
- Danielsson, L. and Ip, W.-H. (1972). Capture Resonance of the Asteroid 1685 Toro by the Earth. *Science*, 176:906–907.
- de la Fuente Marcos, C. and de la Fuente Marcos, R. (2012). Four temporary Neptune co-orbitals: (148975) 2001 XA₂₅₅, (310071) 2010 KR₅₉, (316179) 2010 EN₆₅, and 2012 GX₁₇. *Astronomy and Astrophysics*, 547:L2.
- de la Fuente Marcos, C. and de la Fuente Marcos, R. (2014). Asteroid 2014 OL₃₃₉: yet another Earth quasi-satellite. *Monthly Notices of the RAS*, 445:2985–2994.
- Deprit, A., Jacques, H., Palmore, J., and Price, J. F. (1967). The trojan manifold in the system Earth-Moon. *Monthly Notices of the RAS*, 137:311.
- Edelman, C. (1985). Construction of periodic orbits and capture problems. *Astronomy and Astrophysics*, 145:454–460.
- Gallardo, T. (2006). Atlas of the mean motion resonances in the Solar System. *Icarus*, 184:29–38.
- Giuppone, C. A., Beaugé, C., Michtchenko, T. A., and Ferraz-Mello, S. (2010). Dynamics of two planets in co-orbital motion. *Monthly Notices of the RAS*, 407:390–398.
- Hadjidemetriou, J. D., Psychoyos, D., and Voyatzis, G. (2009). The 1/1 resonance in extrasolar planetary systems. *Celestial Mechanics and Dynamical Astronomy*, 104:23–38.

- Hadjidemetriou, J. D. and Voyatzis, G. (2011). The 1/1 resonance in extrasolar systems. Migration from planetary to satellite orbits. *Celestial Mechanics and Dynamical Astronomy*, 111:179–199.
- Henon, M. (1965a). Exploration numérique du problème restreint. I. Masses égales ; orbites périodiques. *Annales d’Astrophysique*, 28:499.
- Henon, M. (1965b). Exploration numérique du problème restreint. II. Masses égales, stabilité des orbites périodiques. *Annales d’Astrophysique*, 28:992.
- Henon, M. (1969). Numerical exploration of the restricted problem, V. *Astronomy and Astrophysics*, 1:223–238.
- Henon, M. and Guyot, M. (1970). Stability of Periodic Orbits in the Restricted Problem. In Giacaglia, G. E. O., editor, *Periodic Orbits Stability and Resonances*, page 349.
- Jackson, J. (1913). Retrograde satellite orbits. *Monthly Notices of the RAS*, 74:62–82.
- Kinoshita, H. and Nakai, H. (2007). Quasi-satellites of Jupiter. *Celestial Mechanics and Dynamical Astronomy*, 98:181–189.
- Kogan, A. I. (1990). Quasi-satellite orbits and their applications. In *Dresden International Astronautical Federation Congress*.
- Kortenkamp, S. J. (2005). An efficient, low-velocity, resonant mechanism for capture of satellites by a protoplanet. *Icarus*, 175:409–418.
- Kortenkamp, S. J. (2013). Trapping and dynamical evolution of interplanetary dust particles in Earth’s quasi-satellite resonance. *Icarus*, 226:1550–1558.
- Lidov, M. L. and Vashkov’yak, M. A. (1993). Theory of perturbations and analysis of the evolution of quasi-satellite orbits in the restricted three-body problem. *Kosmicheskie Issledovaniia*, 31:75–99.
- Lidov, M. L. and Vashkov’yak, M. A. (1994a). On quasi-satellite orbits for experiments on refinement of the gravitation constant. *Astronomy Letters*, 20:188–198.
- Lidov, M. L. and Vashkov’yak, M. A. (1994b). On quasi-satellite orbits in a restricted elliptic three-body problem. *Astronomy Letters*, 20:676–690.
- Meyer, K. R. and Hall, G. R. (1992). *Introduction to Hamiltonian Dynamical Systems and the N-Body Problem*.
- Mikkola, S., Brasser, R., Wiegert, P. A., and Innanen, K. (2004). Asteroid 2002 VE68, a quasi-satellite of Venus. *Monthly Notices of the RAS*, 351:L63–L65.
- Mikkola, S. and Innanen, K. (1997). Orbital Stability of Planetary Quasi-Satellites. In Dvorak, R. and Henrard, J., editors, *The Dynamical Behaviour of our Planetary System*, page 345.
- Mikkola, S., Innanen, K., Wiegert, P. A., Connors, M., and Brasser, R. (2006). Stability limits for the quasi-satellite orbit. *Monthly Notices of the RAS*, 369:15–24.
- Moeller, J. P. (1935). Zwei Bahnklassen im probleme restreint. *Publikationer og mindre Meddelelser fra Kobenhavns Observatorium*, 99:1–.
- Morais, M. H. M. (2001). Hamiltonian formulation of the secular theory for Trojan-type motion. *Astronomy & Astrophysics*, 369:677–689.
- Namouni, F. (1999). Secular Interactions of Coorbiting Objects. *Icarus*, 137(2):293–314.
- Namouni, F., Christou, A., and Murray, C. (1999). New coorbital dynamics in the solar system. *Physical Review Letters*, 83(13).

- Nesvorný, D., Thomas, F., Ferraz-Mello, S., and Morbidelli, A. (2002). A Perturbative Treatment of The Co-Orbital Motion. *Celestial Mechanics and Dynamical Astronomy*, 82:323–361.
- Robutel, P. and Gabern, F. (2006). The resonant structure of Jupiter’s Trojan asteroids - I. Long-term stability and diffusion. *Monthly Notices of the RAS*, 372:1463–1482.
- Robutel, P., Niederman, L., and Pousse, A. (2015). Rigorous treatment of the averaging process for co-orbital motions in the planetary problem. *ArXiv e-prints*.
- Robutel, P. and Pousse, A. (2013). On the co-orbital motion of two planets in quasi-circular orbits. *Celestial Mechanics and Dynamical Astronomy*, 117:17–40.
- Sidorenko, V. V., Neishtadt, A. I., Artemyev, A. V., and Zelenyi, L. M. (2014). Quasi-satellite orbits in the general context of dynamics in the 1:1 mean motion resonance: perturbative treatment. *Celestial Mechanics and Dynamical Astronomy*, 120:131–162.
- Strömgren, E. (1933). *Connaissance actuelle des orbites dans le problème des trois corps*. *Bulletin Astronomique*, 9:87–130.
- Wajer, P. (2009). 2002 AA₂₉: Earth’s recurrent quasi-satellite? *Icarus*, 200:147–153.
- Wajer, P. (2010). Dynamical evolution of Earth’s quasi-satellites: 2004 GU₉ and 2006 FV₃₅. *Icarus*, 209:488–493.
- Wajer, P. and Królikowska, M. (2012). Behavior of Jupiter Non-Trojan Co-Orbitals. *Acta Astronomica*, 62:113–131.
- Wiegert, P., Innanen, K., and Mikkola, S. (2000). The Stability of Quasi Satellites in the Outer Solar System. *Astronomical Journal*, 119:1978–1984.